Granular Characterization of Stoichiometric Hydroxyapatite Powder Prepared by the Neutralization Method at Neutral pH and Room Temperature

F. Abida, M. Elassfouri, M. Ilou, M. Jamil, B. El ouatli , M. Ezzahmouly, Z.Hatim
Team of Electrochemistry and Biomaterials, Department of Chemistry, Faculty of Sciences,
University of ChouaibDoukkali, El Jadida, Morocco.

Abstract—The precipitation process of the stoichiometric hydroxyapatite in aqueous medium is strongly influenced by the method of preparation and by the operating conditions, and a wide range of apatitic structure of products having calcium / phosphorus ratio and different granular properties can be obtained. This work relates to the characterization of stoichiometric hydroxyapatite powder prepared by the method of neutralization in large quantities at 22°C and at neutral pH. Using the current analysis techniques, we will describe the composition, morphology and dispersion of the grain according to the various preparation steps. The prepared powder formed of nanoscale particles of acicular form, has an atomic ratio Ca/P of 1.664 ± 0.003, a specific surface area of 81.3 ± 0.5m^2/g and a density of 2.923 ± 0.019g/cm^3. The study of the particle size distribution shows an evolution by grow and agglomeration of the fine particles, obtained before drying, to multimodal populations obtained after drying. The heat treatment of the powder shows a dehydroxylation between 950°C and 1300°C and a decomposition to tricalcium phosphate ($Ca_3(PO_4)_2$) and tetra-calcium phosphate ($Ca_4(PO_4)_2O$) at 1450°C.

Index Terms—Stoichiometric hydroxyapatite, Neutralization method, Granular characterization.

1 INTRODUCTION

A NATURALLY occurring form of calcium apatite, hydroxyapatite $Ca_{10}(PO_4)_6(OH)_2$ is an interesting material in Nano technological research. Ranging generally between 80-100nm in size, they are particles that can be dispersed in fluids, made as rods or used as powders for research. Surface functionalized form of Hydroxyapatite powder is also used for preferential binding and adsorption, nuclear waste storage [1], [2], filtration [3] and catalysis [4].The main applications of these materials evidently relate to the field of bone surgery due to the exceptional properties of hydroxyapatite that are : biocompatibility and bioactivity [5]. Indeed, the bioceramics composed of hydroxyapatite knows a great success in the application of covering prostheses deposits on hips or knees [6], [7], [8].

There are a multitude of methods to synthesize hydroxyapatite in pulverulent form [9], [10]: hydrothermal synthesis, solid phase reaction[11], reaction in aqueous phase [12], [13], [14], liquid / solid reaction, Sol gel reaction, synthesis by hydrolysis, synthesis by pyrolysis...

Generally, the technique of precipitation is most commonly used for the preparation of HAP powders on an industrial scale. It is carried out in an ammoniacal medium at basic pH and at elevated temperature by mixing solutions of phosphate ions and calcium ions [16] (reaction (1)).

$$10Ca(NO_3)_2{,}4H_2O+6(NH_4)_2HPO_4+8NH_4OH \rightarrow Ca_{10}(PO_4)_6(OH)_2 + 20NH_4NO_3 + 52H_2O \quad (1)$$

There is another method of neutralization which allows to obtain a non-polluted powder of HAP, the only by-product is water (reaction (2)).

$$10\ Ca(OH)_2 + 6\ H_3PO_4 \rightarrow\ Ca_{10}(PO_4)_6(OH)_2 + 18\ H_2O \quad (2)$$

It is a non-polluting method; the only by-product of the reaction is water, which is very interesting for a preparation on an industrial scale.

The quality of hydroxyapatite powder is estimated by means of its composition of the morphology, size and distribution of grain that is in direct connection with the methods and synthesis parameters.

• *Correspondingauthor: Abida Fatima*
E-mail: abida2007@gmail.com

The aim of our work is the characterization of granular stiochiometric hydroxyapatite powder prepared by the neutralization method in large quantity, at neutral pH and at room temperature.

2 Preparation Method

The synthesis was performed in a reactor, by reaction between calcium hydroxide and orthophosphoric acid. The details of the method are described in our Thesis F [17]. The method used is schematically shown in the flowchart in Figure 1. The solution of orthophosphoric acid was added to the prepared calcium hydroxide slurry. The Ca / P atomic ratio is taken equal to 1.667 (atomic ratio corresponding to a stoichiometric hydroxyapatite).

The reaction is carried out at 22 °C and the precipitation pH is 7 to 7.5. The precipitate obtained is brought to maturation, filtered, and dried at different temperature.

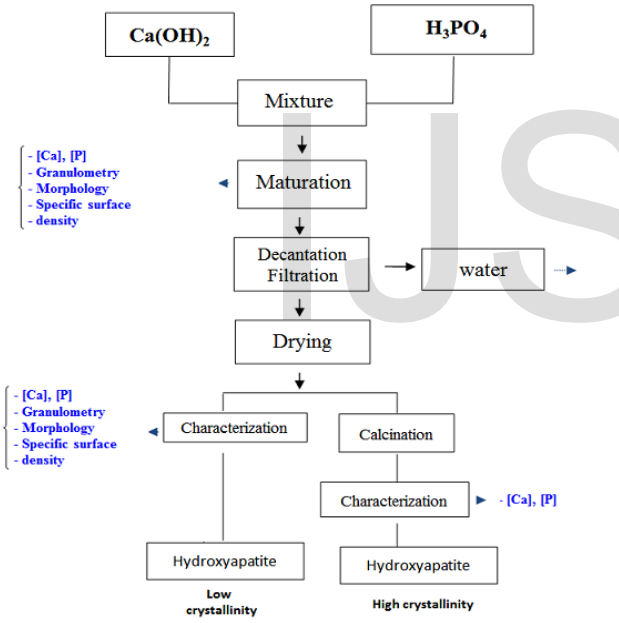

Fig.1: Hydroxyapatite preparationflowchart

3 Characterization Method

The analyses were performed on the powder in suspension, the dried precipitate and on the calcined powder as is shown in Figure 1. During the 636calcinationsan excess of calcium (Ca/P>1.67) results in the presence of calcium oxide, while an excess of phosphorus (Ca/P<1.67) results in the presence of tricalcium phosphate β-type [18]. The phases formed were identified by means of atomic Ca/P ratios, by diffraction analysis of X-rays (D500 Meter, λ_{Cu}=1.5408 Å) and by infrared spectroscopy (Perkin-Elmer FTIR 1600).The structure was refined by the FULLPROF WINPLOTR 2012program[19]. The distribution of grains was measured by laser granulometry (CILAS 920 # 223). The specific surface of the powder was determined by the BET method based on nitrogen adsorption at the surface of the material (Micromeritics ASAP 2010). Morphological analyses were carried out by scanning electron microscope on a device of LeicaSterioscan 430i. The thermal behavior was followed by thermogravimetry (TG), differential thermal analysis (DTA) using a TA Instruments (SDT model 2960)

4 Results and Discussion

4.1. Size and distribution of particles

Analyses of the distribution of the particle size were carried out on the powder in suspension, after filtration and after drying at different temperatures. The results are shown in histograms and cumulative values. Several experiments were performed under the same conditions and have led to the reproducibility of these results.

The results of analyzes of the powder in suspension after 24 hours and 48 hours and after the filtration step do not differ. They show a substantially bimodal particle size distribution (Fig. 2, 3 and 4): a dominant population P2 centered to 5 µm and a secondary population P1 formed of finer grains of the order of 1.4 microns. The grain size is less than 20 µm.

After drying at 60 °C, the results show the disappearance of the secondary population P1, and the appearance of a new population P3 centered to 20 µm (fig.5). After drying at 80 °C, the particle size distribution has three populations (Fig.6): the population P2, population P3 and a new population P4centered around 50 microns. After drying at 105 °C, the distribution became more spread out and multimodal (Fig.7) with a majority population P5centered to 70 µm. In view of these results we can say that the precipitate drying step seems to be important, the fine particles of the powder before drying (populations P1 and P2) grow by agglomeration and give rise to populations P3, P4 and P5.

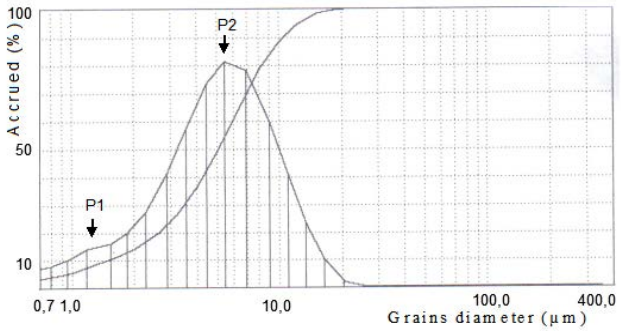

Fig.2: Distribution spectrum of the particle sizeof the powder in suspension after 24 hours of maturation. d0,1=1,53µm, d0,5=5,00µm, d0,9=10.53µm

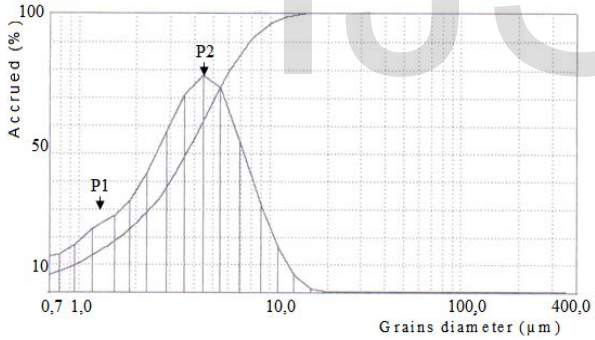

Fig.3:Distribution spectrum of the particle size of the powder in suspension after 48 hours of maturation. d0,1=0,99µm, d0,5=3,64µm, d0,9=7,82µm

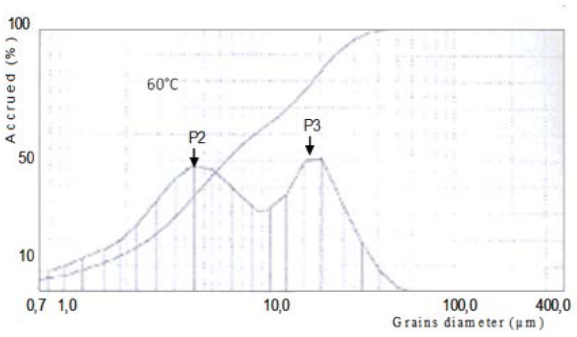

Fig.5: Spectrum distribution of the particle size of the dried powder at 60 ° C.
d0,1=1,49µm, d0,5=6,50µm, d0,9=24,06µm

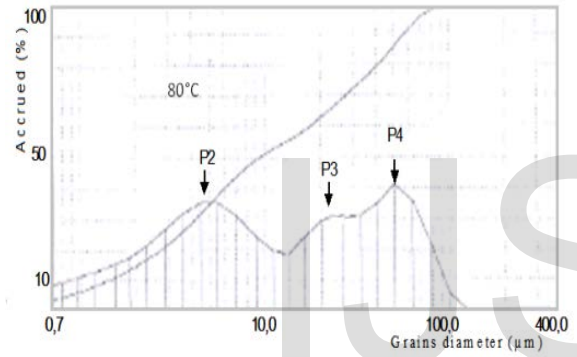

Fig. 6: Size distribution spectrum of the particles of the dried powder at 80 ° C.
d0,1=1,42µm, d0,5=9,35µm, d0,9=58,14µm

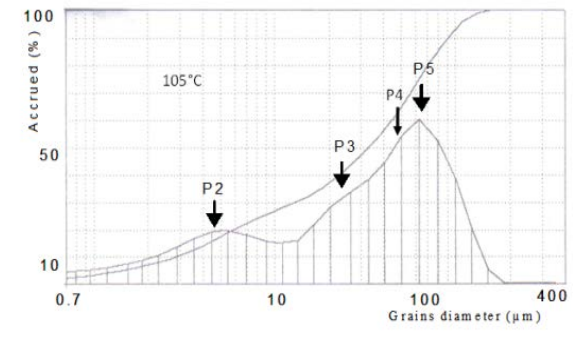

Fig.7: Distribution spectrum of the particles sizeof the dried powder at 105 ° C.
$d_{0,1}$=2,94µm, $d_{0,5}$=33,29µm, $d_{0,9}$=90,28µm

4.2. Specific surface and density of hydroxyapatite particles as a function of the period of maturation

The results of density measurements (Table.1) show values that increase with maturation period indicating a better state of organization. However, these densities remain below the theoretical value of hydroxyapatite (3.16 g/cm^3). The experimental conditions as the supersaturation and the temperature for example, as well as the maturation time do not allow a perfect crystallization of the crystals. The substitution of calcium and phosphorus ions by traces ions can also affect the density of the apatite network.

Table1: Density variation depending on the durationHAP maturation

Maturation (hours)	Specific surface BET(± 0. 5 m^2/g)	Density (g/cm^3)
12	70.5	2.850 ± 0.003
24	81.3	2.923 ± 0.019
48	85.0	2.979 ± 0.003

4.3. Chemical analysis

Chemical analysis was performed on the prepared powder; the results are compared with theoretical values (HAPTHE) (Table. 2). The concentrations of the considered trace ions (Mg, Na, Sr and S) are also shown in this table. The calculated molar ratio of Ca/P of the prepared powder is close to the theoretical value of the stoichiometric hydroxyapatite. Total mass fractionof the trace elements was estimated to612 ppm

Table 2: Maximum concentrations of traces ions detected in the hydroxyapatite powder with above 100 ppm levels.

for the prepared HAP powder. Mg and Sr ions are caused by the calcium carbonate while the Na and S are carried by the orthophosphorique acid and calcium carbonate.

The prepared powder is precipitated at room temperature, at a pH from 7 to 7.5 and in open air which leads to the contamination of the product by the carbonate. The carbonate ions(CO_3^{2-}) are detected with a concentration of 0.3 to 0.5% in weight.

4.4. FTIR analysis

Figure 9(a) shows the Infrared spectrum obtained by the analysis of HAP powder dried at 105°C. The intense bands observed at 900-1200 cm^{-1} and 500-620 cm^{-1} are related to internal vibrations of the PO4 tetrahedra .the presence of bands characteristic of OH groups at 3572 and 3643 cm^{-1} and the presence of the bands located to 1634 and 3433 cm^{-1} attributed to the deformation band HOH corresponding to water molecules trapped in the apatitic network [20].

All the bands observed confirm a poorly crystallized apatite structure. It is also observed the presence of bands to 1450 and 870 cm^{-1} related to $v3CO_3$ and $v2CO_3$apatitic carbonates groups [21]. These carbonate ions come from contamination of the reaction medium with CO_2. The presence of carbonate is confirmed by the chemical dosing (Table.2)

The infra-red spectra of calcined powder (HAP), reported in Figure 9(b), shows on one hand the presence of only one well-crystallized phase of the hydroxyapatite, and, other hand the absence of carbonate and other calcium phosphates such as tricalcium phosphates or calcium oxide.

Sample	Ca (%)	P (%)	Ca/P (Molar ratio)	CO_3 (%)	Mg (ppm)	Na (ppm)	Sr (ppm)	S (ppm)
HAP	38,87 ± 0,54	18,05 ± 0,22	1,664 ± 0,003	0,5	120	180	120	210
HAP_{THE}	39,90	18,50	1,666	-	-	-	-	-

4.5. Morphological analysis

Analyses performed on dry powders at 105°C by scanning electron microscopy SEM highlight the presence of the agglomerates of irregular shape and size of micrometer (fig.11 a).The analysis by transmission electron microscope (Fig.11b) shows that the agglomerates are formed of slightly elongated crystals than a hundred nm in length and fifty nm in diameter and an elongation factor of 2 (table 3). This morphology reflects aciculaire crystallite growth.The Scherrer formula

[22],[23], permitted us to determine the size of the crystals of hydroxyapatite sample prepared in a perpendicular plane to the diffraction plane using the following formula:

$$Lhkl = (0{,}94\ \lambda)/(\cos\theta\ (\Delta r2 - \Delta 02)1/2)$$

With:

0.94: Scherrer constant

L: apparent size in the perpendicular direction in the diffraction plane hkl (Å);

λ : Wavelength of radiation X (copper anticathode λ = 1.5408 Å);

θ: diffraction angle corresponding to the hkl line in question;

Δr : Width at half maximum of a sample diffraction line (radians);

Δ0: Width of the diffraction line of a well crystallized hydroxyapatite (radians).

It was determined on a hydroxyapatite calcined at 900 ° C.

The measurements were carried out on the rays (002) and (310), thus providing information on the crystallite size along the c-axis of the hexagonal cell (line 002) and in a direction perpendicular to the previous (ray 310). On the table 3are reported the apparent dimensions of the crystallites.

The elongation factor obtained (2.024) (table 3) seems smaller than that found in the literature (3 à 5). However, the crystallographic parameters determine d by the FULLPROF WINPLOTR 2012 program [19] (a = 9.4149 ± 0.0003 (Å), c = 6.8755 ± 0.0002 (Å)), are very close to the theoretical values (a = 9.418 (Å) c = 6.884 (Å) [24].

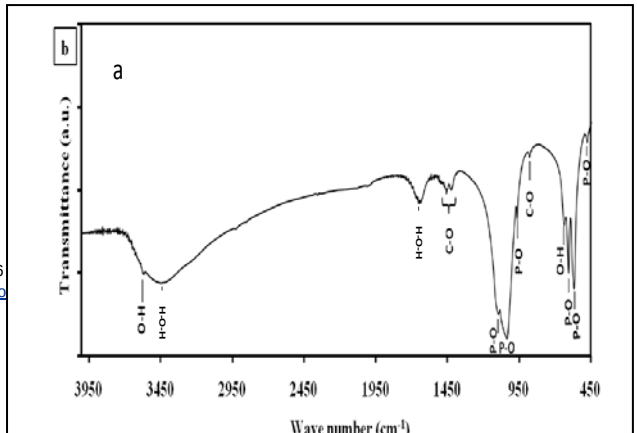

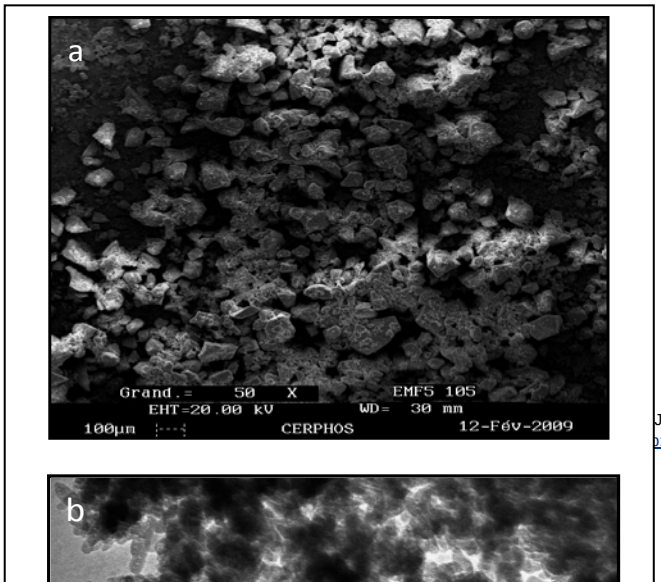

Table 3: Apparent dimensions of theHAP crystallites.

	L(002) ± 5 Å	L(310) ± 5 Å	L(002)/L(310)
prepared HAP	255	126	2.024

1.6. Gravimetric analysis

TGA and DTA measurements on HAP sample reported in Figure 12showed, firstly, weight loss between 950°C to 1300°C

associated with a large endothermic effect, which is characteristic of the HAP dehydroxylation accompanied by formation of oxyapatite according to the reaction (2). The thermal treatment of the products is carried out in air atmosphere where oxyapatite is not stable, in agreement with the literature, the product formed after cooling is hydroxyapatite.

$$Ca_{10}(PO_4)_6(OH)_2 \Leftrightarrow Ca_{10}(PO_4)_6(OH)_{2-2x}O_x + x\,H_2O \quad (2)$$

At 1450°C, the weight loss accelerated strongly and an endothermic peak was observed indicating the HAP decomposition into both tricalcium phosphate ($Ca_3(PO_4)_2$) and tetracalcium phosphate ($Ca_4(PO_4)_2O$) according to the reaction (3). In Figure 13 decomposition of the sample at 1450 °C is confirmed by the XRD analysis.

$$Ca_{10}(PO_4)_6(OH)_{2-2x}\,O_x \rightarrow 2Ca_3(PO_4)_2 + Ca_4(PO_4)_2O + xH_2O \quad (3)$$

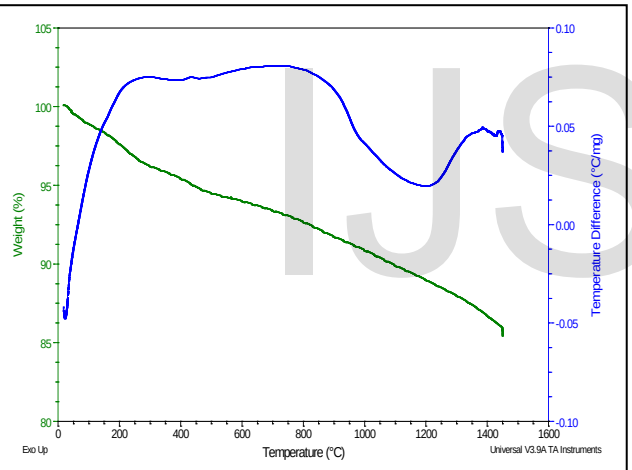

Fig.12: ATD/ATG of trace ions substituted hydroxyapatite powder

structure. According to the Rietveld method with the means of FULLPROF WINPLOTR 2012 program [19].

The structure refinement was performed. The structure of prepared sample was refined considering, as a starting point, the model of theoretical hydroxyapatite (HAP_{THE}) for which we used parameters reported by Sudarsanan and Young [20].Cell parameters are determined and compared to theoretical values (Table 4). Parameters as D_{ind} distortion index, Rc values and volume are gathered in Table 4 and compared to the theoretical values as well. So, the prepared hydroxyapatite crystallized in hexagonal system with unit cell parameters reported in Table 2. Cell parameters (a = b = 9.408 Å, c= 6.872 Å) are slightly lower than those found in theory (a = b = 9.419 Å, c = 6.88 Å).

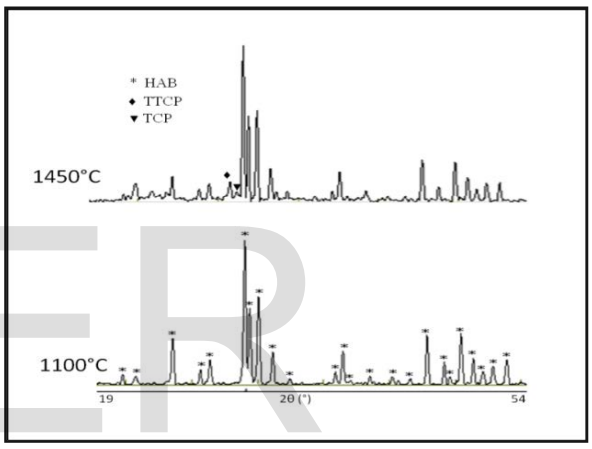

Fig.13:X-ray diffraction patterns of the hydroxyapatite powdercalcined at 1100 °C and 1450°C °C

4.7. X-ray diffraction patterns and Rietveld refinement

X-ray diffraction patterns for both samples HAP are shown in Figure14, confirm the purity of synthetic hydroxyapatite phase calcined at 1100°C. In addition, Rietveld refinement is expected to give more information details about crystalline

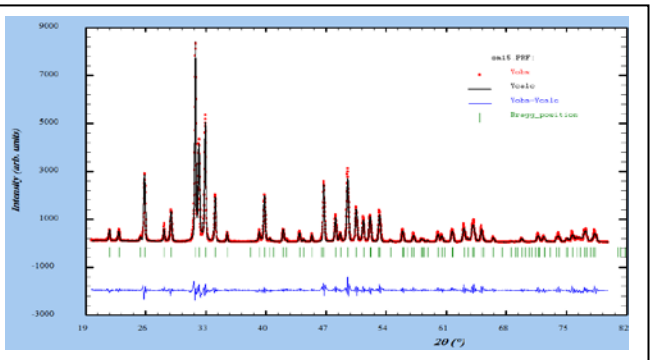

Table 4: Calculated cell parameters.

	HAP	THE(HAP)
a (Å)=b (Å)	9.4079	9.419
c (Å)	6.8720	6.880
α(°)=β(°)	90.000	90.000
γ(°)	120.000	120.000
Spatial group	P 63/m	P 63/m
D_{ind}	3.2043	3.0795
R_c (Å)	1.1778	1.1775
V (Å^3)	526.74	529.16

CONCLUSION

The method of neutralization at room temperature (T = 22°C) and neutral pH, allowed us to obtain the powder of hydroxyapatite stoichiometric Ca/P=1.664 ± 0.003 in great quantities.

The physico-chemical analyzes showed a low crystallinity of the prepared product, the acicular crystal morphology leading to the formation of agglomerates of a large specificsurface and a controlling size of particles.

We have shown that the maturation steps have no significant effect on the particles size distribution while the precipitate drying step appears to be important. Indeed, the crystals finely crystallized from synthesis associate during the drying step to form grains and agglomerates of several microns.The results of the thermogravimetric study show that the prepared powder is stable up to 1450 °C.

REFERENCES

[1] F. Audubert, Mise au point d'une matrice apatitique pour le confinement de l'iode 129, thèse, Institut National Polytechnique de Toulouse, 1995.
[2] J. Carpena, J-L. Lacout. L'Actualité Chimique, 2 (1997) 3-9.
[3] F. Yang, B. Shi, F. Meng, H. Zhang. Environmental Progress, 26(1) (2007) 86–93
[4] J. C. Elliot. Amsterdam: Elsevier, 18(1994).
[5] Brevet Européen WO 2005/004942.
[6] K. DE GROOT, C. P. T. A. KLEIN, Calcium phosphate bioceramics: their future in clinical practice, Biomaterials degradation: fundamental aspects and related clinical phenomena, Eur. Mat. Res. Sos. Monogr., Ed. Barbosa, North-Holland, 1, 169-185, 1991.
[7] K. A. Thomas. Orhtopedics, 17 (3) (1994) 267-278.
[8] R. MC PHERSON, N. GANE, T. J. BASTOW. Materials in Medicine, 6 (1995) 327-334.
[9] R. A. YOUNG, D. W. HOLCOMB. Calcified Tissue International, 34, S17-S32, 1982.
[10] J. ARENDS, J. Christoffersen, M. R. Christoffersen, H. Eckert, O. Fowler, J.C. Heughebaert, G. H. Nancollas, J. P. Yesinowski, S. J. Zawacki. Journal of Crystal Growth, 84(1987) 515-532,.
[11] R. Ramachandra Rao, H.N. Roopa, T.S. Kannan. J. Mater. Sci. Mater. Med., 8(1997)511-518.
[12] S.H. Rhee, J. Tanaka. J. Am. Ceram. Soc., 81 (1998) 3029-3031.
[13] A. Jillavenkatesa, R.A. Condrate SR. J. Mater.Sci., 33 (1998) 4111-4119.
[14] H.K. Varma, S.N. Kalkura, R. Sivakumar. Ceram. Int., 24 (1998) 467-470.
[15] K. Yamashita, T. Arashi, K. Kitagaki, S. Yamada, T.Umegaki. J. Am. Ceram. Soc., 77(9) (1994) 2401-2407.
[16] N. MONMATURAPOJ. Journal of Metals, Materials and Minerals, 18(1) (2008) 15-20.
[17] F. Abida, Ph.D, UCD, Maroc, 2011.
[18] AFNOR, NF S 94-066, AFNOR Paris (1998).
[19] J. Rodriguez-Carvajal. Physica B, 192 (1993) 55-69.
[20] K. Sudarsanan, R.A. Young. Acta Crystallographica B, 25 (1969) 1534-1543.
[21] J. Lafon, Thèse. Université de Limoge, France 2004.
[22] P. Scherrer, GöttNachr 2 (1918) 98.
[23] M.J. GLIMCHER, L. C. Bonar, M.D. Grynpas, W.J. Landis, A. H. Roufosse. J. Crystal Growth, 53 (1981) 100-119.
[24] M. I. KAY, R. A. YOUNG, A. S. POSNER. Nature, 204 (1964) 1050-1052.